

Effect of bed friction on morphodynamic modelling: Application to the central part of the Gironde estuary

C. Villaret & J.M. Hervouet

EDF R&D—Laboratoire National d'Hydraulique et Environnement (LNHE), Saint Venant Laboratory for Hydraulics, Université Paris Est (joint research unit EDF R&D—CETMEF—Ecole des Ponts ParisTech), Chatou, France

N. Huybrechts & L.A. Van

Saint Venant Laboratory for Hydraulics, Université Paris Est (joint research unit EDF R&D—CETMEF—Ecole des Ponts ParisTech), Chatou, France

A.G. Davies

School of Ocean Sciences, Bangor University, Menai Bridge, UK

ABSTRACT: A 2D depth-integrated morphodynamic model has been applied to simulate 10 years of bed evolution in the central part of the Gironde macro-tidal estuary. The effect of friction on both hydrodynamics and sediment transport has been illustrated in this complex environment. Different values of the Strickler coefficients, ranging from flat bed to dune regimes, have been compared in order to reproduce both the free surface elevation and mean flow velocity measurements. For sand transport rate predictions, Van Rijn's (2007) formulation has also been implemented in order to predict the rippled bed roughness.

1 INTRODUCTION

In rivers, littoral or estuarine environments, the need of reliable morphodynamic predictions has inspired many researchers to build numerical tools of different complexity from 2D to complete 3D models. In the so-called process models, a detailed representation of hydrodynamics is required in order to calculate the sediment transport rates including both bed-load and suspended load and the resulting bed evolution (see a review for example in Papanicolaou, 2008).

For a number of applications, the 2D depth-integrated approach can give a first representation of a relatively simple situation (without stratification effects). For medium term bed evolution of the order of decades, on mid-scale domains (a few tens of kms), this approach is a good compromise, which allows a detailed representation of the coupling between hydrodynamics and sand transport processes.

For modelling purposes, it is necessary to parameterize the spatially variable bed roughness as a single length, representative of the variability of bed forms within one grid scale.

The bed roughness enters the momentum equation, through some classical friction laws (e.g. Strickler friction). For the flow model, the bed roughness and

associated friction coefficient can generally be used as a calibration coefficient, in order to represent the mean flow variables (water level and velocity field). For the sediment transport model, this approach is however not sufficient, since sediment transport predictions are generally highly sensitive to the local skin friction, which represents the part of friction acting locally on individual grains.

The objective of this paper is to illustrate the sensitivity of model predictions to the bed roughness and associated friction coefficients, which are considered as main source of uncertainty in the 2D approach. This is illustrated in the case of the Gironde macro-tidal estuary where drastic bed evolutions have been observed in the central portion of the estuary, characterized by the presence of channels and banks (Chini and Villaret, 2007). We use here the Telemac finite element system, with internal coupling between the hydrodynamic flow model (Telemac 2D) and the morphodynamic model (Sisyphé), developed at EDF R & D (cf. Hervouet, 2007, Villaret, 2005). We allow here the use of different friction coefficients for both hydrodynamic and morphodynamic models. A skin friction predictor, based on Van Rijn (2007), has been implemented in order to improve the accuracy of the sand transport calculations.

2 THEORETICAL BACKGROUND ON THE ROLE OF FRICTION

2.1 Bed roughness decomposition

The presence of bedforms, from small scale ripples to dunes, has a large effect on the near bed velocity profile and bed shear stress, as reported in laboratory experiments and modelling work. This effect can be parameterized for modelling purposes by a single length scale, the equivalent bed roughness, which can be related to bedform dimensions and sand grain diameter.

According to Van Rijn (1984), the bed roughness k_s can be decomposed into a grain roughness k'_s and a drag roughness component k''_s , due to bedforms.

$$k_s = k'_s + k''_s \quad (1)$$

The grain roughness is proportional to the mean grain size d_{50} , with $k'_s = 2-3d_{50}$ for fairly uniform grains, or to the larger grain size d_{90} , $k'_s = 3d_{90}$ for non uniform grains.

According to Van Rijn (2007), the form drag is due to the energy loss in the lee of bedforms, including ripples, mega-ripples and dunes.

$$k''_s = \sqrt{k_r^2 + k_{mr}^2 + k_d^2} \quad (2)$$

where k_r is the roughness of small scale ripples, k_{mr} , the bed roughness of mega-ripples and k_d the dune roughness.

Each component can be related to the mobility number ψ , which, for the current dominated regime, can be defined in terms of the time-varying depth-averaged mean flow velocity, U , relative density $\Delta = 1.65$, gravity g and mean grain diameter d_{50} .

$$\psi = \frac{U^2}{\Delta g d_{50}} \quad (3)$$

2.2 Effect of total friction on the mean flow

Hydrodynamic variables (spatially-averaged over bedforms) depend on the total friction which enters the 2D depth-averaged momentum equation, in addition to the pressure term and other source terms.

In the 2D approach, the bottom shear stress τ_0 is related to the depth-averaged velocity U . Here, we use a Strickler coefficient, denoted S_f ($m^{1/3} s^{-1}$):

$$\tau_0 = \rho \frac{g}{S_f^2} \frac{1}{h^{1/3}} U \quad (4)$$

where g is gravity, h the water depth, and ρ the fluid density.

The Strickler coefficient can be related to the equivalent bed roughness k_s . Eq (5) can be obtained by integrating over depth the classical logarithmic velocity profile, assumed to be valid up to the free surface.

$$S_f = \frac{\sqrt{g}}{\kappa} h^{-(1/6)} \ln \left(\frac{11h}{k_s} \right) \quad (5)$$

where $\kappa = 0.4$ is the von Karman constant.

The bed roughness can be predicted from the flow variables for different regimes, from plane beds to dunes (Yalin 1977, Van Rijn 1984). However, bed roughness predictors from the literature have been established assuming equilibrium conditions and are mostly valid under steady flow conditions. Their validity in complex field conditions, in an unsteady tidally dominated regime, is therefore questionable.

However, considering the various sources of uncertainty in the validity of bed roughness predictors, the friction coefficient is generally considered as a calibration coefficient, and is part of the various sources of uncertainty in the flow model, including side friction effects.

2.3 Effect of skin friction on sand transport rates

We assume here the classical partition of sand transport rates into bed-load and suspended load. Bed-load transport rates are calculated as a function of skin friction, by using a semi empirical formula (e.g. Meyer-Peter and Muller, 1948). For the suspended load, an additional transport equation is solved for the sediment concentration, where source terms (erosion flux) are expressed as a function of an equilibrium concentration, which is also calculated using a semi-empirical formula as a function of skin friction (e.g. Zyserman and Fredsoe, 1994). The skin friction τ_s is therefore the main hydrodynamic parameter, which influences both bedload and suspension.

According to Bijker (1992), the drag component of the bed shear stress generated by small scale ripples, denoted τ_r , should contribute to transport rate calculation. Therefore, the skin friction τ_s , should be a combination of the ripple-generated bed shear stress τ_r and grain roughness generated friction τ' :

$$\tau_s = \left(\frac{\tau'}{\tau_r} \right)^\alpha \tau_r \quad (6)$$

with $\alpha \sim 0.75$.

Another possible formulation would be to take $k'_s = \max(3D_{90}, k_r)$.

The ripple bed roughness can be predicted from the flow variables, assuming equilibrium conditions. According to Van Rijn (2007), the ripple induced bed roughness can be predicted as a function of the

mobility number, where ψ is defined by (3), as follows: for $\psi < 250$

$$k_r = d_{50} \{85 - 65 \tanh [0.015 (\psi - 150)]\} \quad (7)$$

and for $\psi > 250$: $k_r = 20 d_{50}$

2.4 Methodology for the determination of friction coefficients

We allow the use of two different friction coefficients, the first one for the hydrodynamic model and the second one for the sediment transport model.

In the hydrodynamic model, the friction coefficient should represent the total friction and include the variability in bed forms. In theory, the total friction coefficient should be linked to the observed or predicted dimensions of bedforms. However, there is generally a lack of detailed observations of the time varying and spatial distribution of bedforms under field conditions. In the literature, predictors of bedforms have been obtained in idealized conditions (steady uniform flow, uniform sand) and their validity in complex field conditions is questionable.

It is assumed, as a first approach, to use the hydrodynamic model friction coefficient as a fitting coefficient in order to reproduce the flow observations (depth-averaged velocity and free surface variation). For the sand transport model, there is generally a lack of direct measurements of sand transport rates, which could be used to calibrate the value of the skin friction coefficient. In the absence of data, the Van Rijn equation (7) can be used to predict the ripple roughness. The small scale bedforms are indeed believed to adapt rapidly to the time-varying flow, such that equilibrium relations should be valid, even in a tidally dominated signal.

3 MODELLING THE CENTRAL PART OF THE GIRONDE ESTUARY

3.1 Presentation of site and previous work

The sensitivity of model predictions (both hydrodynamics and morphodynamics) and the proposed methodology for bed friction determination are illustrated here in a complex environment: the central part of the Gironde macro-tidal estuary, with tidal amplitude ranging from 5 to 8 m. The bathymetry data surveys from 1995 to 2005 show a drastic evolution leading to a slow fill-up of secondary channels, separated from the main channels by elongated sand banks.

The 2D model is based on previous work by Chini and Villaret (2007) and includes optimization in the flow-sediment transport methodology, which allows the use of larger time steps, and makes it now possible to compute ten years of bed evolution with reasonable CPU time. The model assumptions (2D, uniform

sand grain) do not account for stratification effects nor for the presence of mud and sand-mud mixture. The effect of dredging and release in this zone has not been included.

3.2 Hydrodynamic and sediment transport models

Hydrodynamics is computed by Telemac-2D, which solves the 2-dimensional Saint Venant or shallow water equations, on unstructured grids. Its solution procedure, based on the finite element technique, is fully detailed in Hervouet (2007). We have chosen here to use the wave equation option, which broadly consists of eliminating the velocity from the continuity equation, with the help of the momentum equation, to get the water depth in a first fractional step, and then to retrieve the velocities from the momentum equation once the depth is known. Large Courant numbers are allowed and dry zones can be included in the model. At every time step, i.e. every 150 s in this application (central part of the Gironde estuary), depth-averaged velocity, depth and friction are transmitted to the morphodynamic model (Sisyphé), which computes the bedload and the suspended sediment transport. Sisyphé solves the Exner equation, which is extended to account for erosion and deposition due to suspended sediment, in order to get the bed evolution. The updated bed elevation is sent back to Telemac-2D for the next time step. This procedure is now used for all our applications.

For this application, two embedded models have been built, as shown in Figure 1. The first model, referred to as the larger model, with 12 552 points,

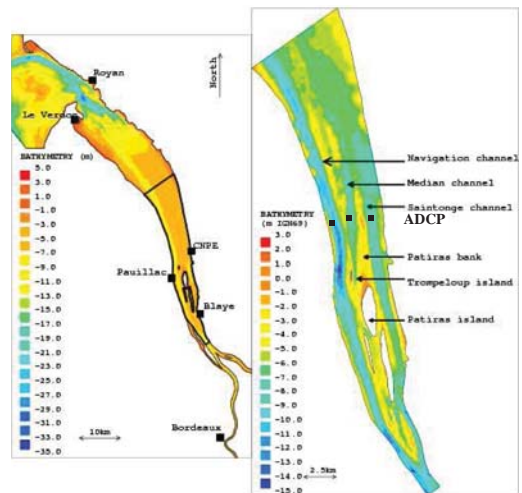


Figure 1. Location map—The figure on the left represents the large scale model (150 km) and the figure on the right the local model of the central part (40 km).

covers all the Gironde estuary, including large reaches of the tributaries. It is forced by the tidal boundary conditions in the North, and by the discharges of rivers in the South. 14 tidal waves are considered, amplitudes and phases were provided by the Service Hydrographique et Océanographique de la Marine (SHOM), see Roy and Simon 2003. These amplitudes and phases basically reproduce the tide of 1st January 1900, and phase shifts may be introduced to get the tide of any other given date. In the larger model, no bed evolution is considered. The second model, referred to as smaller model, covers 40 km of the central part of the estuary, from PK 30 to PK 70. It contains 11 500 points, including 33 points on the open boundaries, whose boundary conditions will be given by the larger model. For this smaller model, Telemac-2D is run in a coupled way with Sisyphe to get the bed evolution.

3.3 *Boundary conditions and model coupling*

We have a fluvial regime in the Gironde estuary, and the theory of characteristics for shallow water equations states that only one boundary condition may be prescribed at open boundaries, either depth or velocity, or, if we apply strictly the theory, a Riemann invariant which is a combination of both depth and velocity. This latter option, known as the Thomson's method in Telemac-2D, was tested but was eventually discarded because it did not allow control of the exact discharge that was injected in the smaller model. The retained procedure for the boundary conditions is the following:

- when the flow exits at an end of the smaller model, the elevation given by the larger model is prescribed. The velocity is free and is treated as a degree of freedom.
- when the flow enters at an end of the smaller model, the total discharge given by the larger model is prescribed. The elevation is free and is treated as a degree of freedom.

As the discharge is not a sufficient condition for an upstream boundary, a velocity profile proportional to \sqrt{h} , where h is the depth, is assumed. This seemingly complicated procedure is due to the fact that the bed evolves in the small scale model, but not in the larger, which may lead to different velocity profiles. Our depth-dependent profile, which is derived from the Chézy law for permanent and uniform flows, is close to physics and ensures that no velocity will be prescribed on a dry bed. This choice was retained because tests with prescribed velocity profiles taken from the larger model proved to give abnormal bed evolutions at the boundaries. Special care must also be given to the sediment boundary conditions. When the flow exits from the domain, the concentration of

suspended sediment is a degree of freedom and is naturally derived from the knowledge of the concentration inside the domain. When the flow enters the domain, the concentration coming from outside is unknown and an assumption must then be made. We assume here equilibrium concentration and bed load transport rates, such that there is no evolution. This condition happens to be a strong limitation of embedded models for sediment transport and could be responsible for abnormal erosion or deposition on the boundaries.

For a time step of 150 s, the computer time is about 3 days on a Intel Xeon 2.33 GHz linux station for a ten year bed evolution, using parallel calculation on 2 processors.

4 TOTAL BED ROUGHNESS AND HYDRODYNAMIC MODEL VALIDATION

4.1 *Observations (bedforms and granulometry)*

Velocity profiles have been measured in August 2006, using ADCP, at three points located in different channels in the same cross-section than the EDF nuclear power plant, called CNPE (see location map in figure 1). Measurements of the free surface variation are also available at the harbour of Pauillac. The tidal amplitude ranges from 2.5 m to 4.5 m, whereas the velocity is larger in the main navigation channel (up to 1.5 m/s).

Granulometry distributions are highly variable and most samples show bi-modal distributions typical of a sand/mud mixture (Boucher, 2009). For the non-cohesive fraction, the grain size is made of fine sands, with a mean grain size of $d_{50} = 210 \mu\text{m}$ (see Chini, 2007). The presence of large scale bedforms has been reported in the right handed channel, upstream of the power plant (Oliveira, 2009, personal communication). Typical dimensions of those small scale dunes are about 5.5 m in length with a height of approximately 70 cm (+/-20 cm).

4.2 *Choice of Strickler coefficient*

According to Eq. 5, a Strickler coefficient of about 75 corresponds to the grain roughness, whereas a Strickler value close to 50 is reached for a bed roughness of a few centimetres, as typically met with rippled bed. On this topic, we should also note that a value of 100 is generally associated with the roughness of a smooth glass wall. A constant Strickler coefficient in the range [25–75] has been assumed in order to represent different realistic bed configuration from dunes, to rippled or flat bed.

In order to validate this assumption, the Van Rijn (2007) formula for total roughness (eq. (1), via (2) and (7)) has been applied using the data collected at the three points in August 2006, on which the optimal value of the Strickler has been extracted, using (5).

The Van Rijn formula predicts a local flow configuration of duned or rippled bed. Indeed, the total bed roughness variation during one tidal cycle reaches a maximum value of 30 cm (Fig. 2) and the associated Strickler coefficient rather ranges between 30 and 45. The time variability of the predicted bed roughness is probably overestimated, since the Van Rijn equilibrium formula does not take into account the adaptation time scale of large scale bedforms.

More bed observations are needed to determine if the bed configuration corresponds locally (at the measurement points) and on average along the grid scale to either a flat-rippled bed or a rippled-duned bed and to assess the efficiency of equilibrium bed roughness predictor under a tidal flow regime.

The presence of clay material may also lead to a drag reduction (Gust 1976; Wang et al. 1998). The agglomeration of clay may exhibit long chain structures which can suppress the development of turbulence near the bottom (Wang et al. 1998) similarly to the drag reduction obtained when adding polymers (Toms effect).

4.3 Sensitivity of hydrodynamic model to the Strickler friction coefficient

In order to assess the influence of the friction term, three computations only involving the hydrodynamic model have been carried out with different values of the Strickler coefficient: 25, 50 and 75.

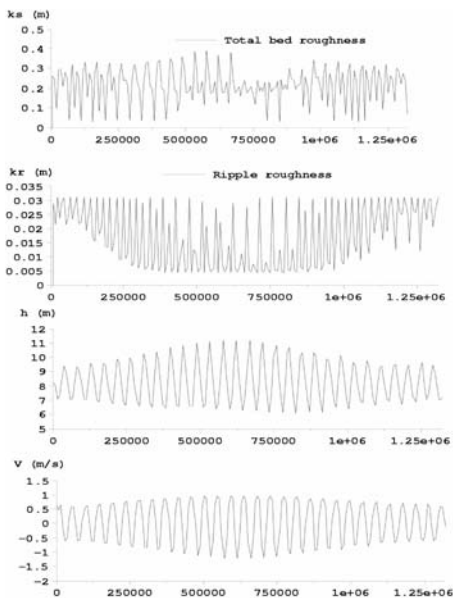


Figure 2. Van Rijn (2007) predictor of bed roughness (ripple skin friction and total roughness) at measurement point 2 (right handed channel).

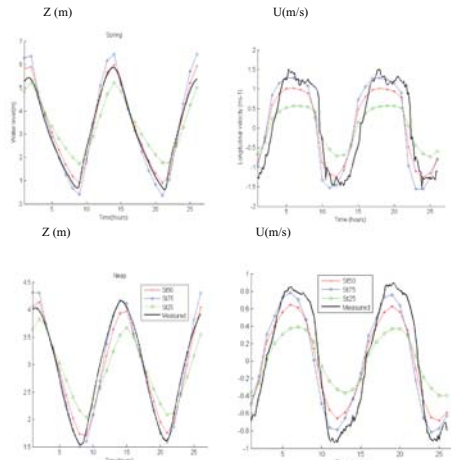


Figure 3. Effect of Strickler coefficient on the variation of the free surface at Pauillac (figures on the left) and on velocity (figures on the right). The top figures represent spring tidal conditions and the bottom ones, neap tide.

The comparison between the numerical results and the measurements are plotted in Figures 3, for both neap and spring tides. For the water depth at Pauillac station, the numerical results follow the measurements more correctly with $S_t = 50$. Near the power plant, best agreements are observed with $S_t = 75$ for the velocity and $S_t = 50$ for the water depth.

In the morphodynamic model simulation presented below, we apply a constant Strickler coefficient of 50, for the hydrodynamic model, which gives an overall good agreement, although the numerical results could be improved by using a time-varying and spatially-varying Strickler value. The calibrated constant value of Strickler ($S_t = 50$) differs from the predicted value using the Van Rijn (2007) formula ($S_t = 35-40$), whose efficiency needs to be further evaluated in the Gironde estuary.

5 SKIN FRICTION AND MORPHODYNAMIC MODEL VALIDATION

The sand transport model has been here internally coupled to the hydrodynamic flow (using previous calibrated value of the Strickler coefficient $S_t = 50$) and applied to simulate the bed evolutions observed during the period from 1995 to 2005. The bathymetric measurements made by the Port Authority of Bordeaux have been interpolated on the triangular grid of the small scale model (11 500 nodes). Measured bed evolutions are shown in Figure 4.

The Van Rijn (2007) formula for ripples has been implemented in order to predict the value of skin (ripple) friction (Van Rijn model, 2007). As shown in

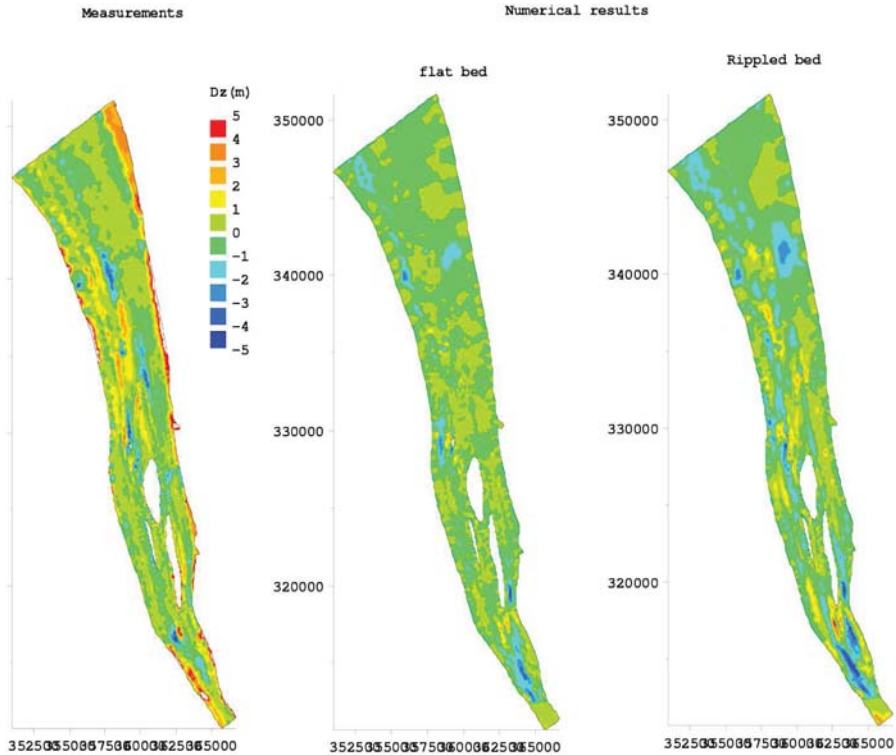


Figure 4. Effect of skin friction on the bed evolution from 1995 to 2005. Measured bed evolutions are shown on the left. The central figure shows the morphodynamic model results, assuming flat bed and the right figure corresponds to rippled bed.

Figure 2, at a point located here in the middle of the channel on the right, the skin friction varies during the tidal cycle from typical flat bed conditions of a few mms to typical ripple roughness of about 3 cm.

We first assume constant skin friction and show how much the transport rates by both bedload and suspended load are enhanced in comparison to flat bed conditions.

The effect of skin friction on the bed evolution is also shown in Figure 4: the bed evolution is enhanced when the bed roughness is larger. Best agreement between model predictions and measurements is obtained by including the bed roughness predictor. Measurements and model results are now of the same order of magnitude, although there are still some discrepancies, probably due to neglected processes.

6 CONCLUSIONS

The internal coupling between Telemac-2D and the morphodynamic model (Sisyphé) has been applied to simulate 10 years of bed evolution in the central part of the Gironde macro-tidal estuary.

In this paper, the effect of friction on both hydrodynamics and sediment transport has been illustrated, and model results (free surface, velocity and bed evolutions) have been compared with measurements. The friction coefficient represents the variability in the bedforms averaged over one grid scale, and the predictive capacity of existing models for the bed roughness in this complex environment (macro-tidal estuary, effect of cohesive sediments) has been discussed.

Different values of the Strickler coefficients, ranging from flat bed to dune regimes, have been compared in order to reproduce both the free surface elevation and mean flow velocity measurements. For sand transport rate predictions, the Van Rijn (2007) formula has also been implemented in order to predict the ripple bed roughness.

Morphodynamic model predictions have been improved by including the Van Rijn bed roughness predictor. Some discrepancies between measurements and numerical results are observed near the upstream and downstream boundaries due probably to the coupling procedure between the large scale and local model. Other improvement could be achieved by taking into accounting the variability in the Strickler

coefficient in the hydrodynamic model and also for the presence of mud which is dominant in the central part of the estuary.

ACKNOWLEDGEMENTS

This work is part of the PhD thesis of Lan Anh Van, which benefits of a partial funding of the Cetmef, French Ministry of Ecology. Observations of bed-forms were made by Eric de Oliveira (Edf R & D) and measurements of granulometry distribution by Olivier Boucher under the supervision of Damien Pham Van Bang from Cetmef are acknowledged.

REFERENCES

- Bijker E.W. 1992. Mechanics of sediment transport by the combination of waves and current, In *Design and Reliability of Coastal Structures, 23rd Int. Conf. on Coastal Engineering*, 147–173.
- Boucher O. 2009. Rapport technique sur les analyses granulométriques des sédiments Girondins à proximité de la CNPE du Blayais, 20 p. (in French).
- Chini N. and Villaret C. 2007: Numerical modeling of the bed evolution downstream of a dike in the Gironde estuary, *Proceedings of the River, Coastal and Estuarine Morphodynamics Conference*.
- Gust, G. 1976. Observations on turbulent-drag reduction in a dilute suspension of clay in sea water. *Journal of Fluid Mechanics*, 75(1), 29–47.
- Hervouet, J.M. 2007. Hydrodynamics of free surface flow, finite elements system. Wiley.
- Le Roy, R. and Simon, B. 2003: Réalisation et validation d'un modèle de marée en Manche et dans le Golfe de Gascogne- Application à la réalisation d'un nouveau programme de réduction des sondages bathymétriques. *Rapport d'étude SHOM n°002/03*.
- Meyer-Peter, E. and Muller, R. 1948: Formulas for bed load transport. *Proceedings of the 2nd Meeting of the International Association of Hydraulic Research*, Stockholm, 39–64.
- Papanicolaou, N. and Elhakeen, M. et al. 2008: Sediment transport modeling Review, Current and Future development, *Journal of Hydraulic Engineering*, 134(1).
- Van Rijn, L.C. 1984. Sediment transport, part III: bed forms and alluvial roughness. *Journal of Hydraulic Engineering*, 110(12), 1733–1754.
- Van Rijn, L.C. 2007. Unified view of sediment transport by currents and waves. 1. Initiation of motion, bed roughness, and bed-load transport. *Journal of Hydraulic Engineering*, 133, 6, 649–667.
- Villaret, C. 2005. Sisyphé release 5.5—User manual, *EDF-LNHE report HP76/05/009*.
- Wang, Z.Y., Larsen, P., Nestmann, F. and Dittrich, A. 1998. Resistance and drag reduction of flows of clay suspensions. *Journal of Hydraulic Engineering-Asce*, 124(1), 41–49.
- Yalin, M.S. 1977. Mechanics of sediment transport, Pergamon Press, 2 Ed., Oxford, 298 p.
- Zyserman, J. and Fredsoe J. 1994: Data Analysis of Bed Concentration of Suspended Sediment, *Journal of Hydraulic Engineering*, 120(19), 1021–1042.

